given for peak-height or area measurement of amide S as well as of amide II with which α-helical content can be determined for any protein.

Acknowledgment. We thank Doctors G. Stockton and P. Mowery, American Cyanamid Company, for a sample of bovine somatotropin and Professors S. Krimm and S. Asher for stimulating discussions and for communicating the results of their work prior to publication. This work was supported by NIH Grant GM 12528.

UVRR Spectroscopy of the Peptide Bond. 2. Carbonyl H-Bond Effects on the Ground- and Excited-State Structures of *N*-Methylacetamide

Yang Wang, Roberto Purrello,† Savas Georgiou,‡ and Thomas G. Spiro*

Contribution from the Department of Chemistry, Princeton University, Princeton, New Jersey 08544. *Received July 23, 1990*

Abstract: Ultraviolet resonance Raman (UVRR) spectra of *N*-methylacetamide (NMA) are markedly solvent dependent. When non-H-bonding solvents are compared with water, the amide I band is seen to intensify and shift up in frequency, while the amide II, III, and S bands weaken and shift down in frequency. The amide I frequency is linearly correlated with the solvent acceptor number (H-bond donating tendency), while the N–H stretching infrared frequency is linearly correlated with the solvent donor number (H-bond accepting tendency), but there is no cross-correlation. Thus, the ground-state structure of the amide bond is sensitive to C=O but not to N–H H-bonding. Raman excitation profiles (EPs) in water show maxima at the first allowed absorption maximum, 188 nm, for amide II, III, and S but not for amide I, which shows only preresonance enhancement from a transition at ca. 165 nm. In acetonitrile, the intensity order is amide I > III > II > S, and the EPs all rise strongly toward the blue-shifted first absorption maximum. These dramatic changes are suggested to arise from stabilization of the C=O π^* fragment orbital by H-bonding, resulting in an altered orbital pattern and lowered energy for the first π–π^* excited state. In stationary samples, a 1495-cm^{-1} band grows in with increasing laser power. It is assigned to the amide II band of the *cis*-amide isomer by comparison with the UVRR spectrum of the cyclic *cis*-amide, caprolactam. At laser powers sufficient to convert 20% of the NMA to the cis isomer, the Stokes/anti-Stokes intensity ratio of an 831-cm^{-1} probe band of deuterated acetonitrile revealed a temperature rise within the scattering volume of 25 °C, sufficient to account for an increase of only 1% in the cis isomer fraction via heating. Most of the isomerization is therefore induced by photoexcitation. MINDO/3 calculations of the potential with respect to twisting about the C–N bond show a minimum energy for the S_1 state at 90°, suggesting a facile pathway for photoisomerization. The photoisomerization yield is much higher in water than in acetonitrile, an effect attributable to a deeper excited-state potential well, due to the same orbital changes that account for the altered EPs. The yield also decreases with steric bulk of substituents on the amide C and N atoms, as expected from steric clashes in the 90° twisted geometry. Photoisomerization is seen for glycylglycine but is barely detectable for glycyllysine and alanylalanine. For hexaglycine, the photoisomerization yield, per amide bond, is only about 40% of that seen for glycylglycine, suggesting that only the outer two of the five amide bonds are affected. Consequently, photoisomerization is expected to be unimportant for polypeptides and proteins except for terminal glycine residues. The overtone of the amide V out-of-plane N–H bend is not observed in NMA UVRR spectra, even directly on resonance at 192 nm. The low enhancement is suggested to reflect a relatively shallow slope for the S_1 twisting potential or a small degree of twist in the amide V normal coordinate.

Introduction

N-Methylacetamide (NMA) is the simplest realistic model compound for the peptide bond. Its ultraviolet resonance Raman (UVRR) spectrum has recently been examined in connection with the development of UVRR probes of protein structure.[1-7] These studies revealed enhancement of amide vibrational bands near resonance with the strong 190-nm absorption band assigned to the first π–π^* transition, as expected, but they also contained surprises, which have prompted the present investigation. Thus, Hudson and co-workers found strong enhancement of the carbonyl stretching mode, amide I, in the vapor phase or in acetonitrile solution, but could not detect the band in aqueous solution.[1,2] They suggested that a distribution of H-bonded structures in water might broaden the amide I band out of recognition. In the present study, we examine the UVRR spectra of NMA in various solvents and find that amide I is hidden by amide II in aqueous solution, because H-bonding solvents shift the frequencies of these modes in opposite directions and also reverse their intensities. Both of these effects can be understood on the basis of H-bond influences on the amide resonance structures or, equivalently, on the HOMO/LUMO orbital compositions. Interestingly, the H-bond effect on the amide electronic structure is due exclusively to interactions at the carbonyl group and not at the N–H group.

* Author to whom correspondence should be addressed.
† Present address: Dipartimento di Scienze Chimiche, Università di Catania, Viale A. Doria, 6, 95125 Catania, Italy.
‡ Present address: Alketou 8 Str., Pagrati, Athens, Greece.

(1) Mayne, L. C.; Ziegler, L. D.; Hudson, B. *J. Phys. Chem.* **1985**, *89*, 3395–3398.
(2) Mayne, L. C.; Hudson, B. *Proceedings of the 11th International Conference on Raman Spectrocopy*; Clark, R. J. H., Long, D. A., Eds.; John Wiley & Sons: New York, NY, 1988; p 745.
(3) Dudik, J. M.; Johnson, C. R.; Asher, S. A. *J. Phys. Chem.* **1985**, *89*, 3805–3814.
(4) Harada, A. I.; Takeuchi, H. *Spectroscopy of Biological Systems*; Clark, R. J. H., Hester, R. E., Eds.; John Wiley & Sons: New York, NY, 1986; pp 113–175.
(5) (a) Song, S.; Asher, S. A.; Krimm, S.; Vandekar, J. *J. Am. Chem. Soc.* **1988**, *110*, 8548–8550. (b) Krimm, S.; Song, S.; Asher, S. A. *J. Am. Chem. Soc.* **1988**, *111*, 4290.
(6) Song, S.; Asher, S. A.; Krimm, S.; Shaw, K. D. *J. Am. Chem. Soc.* In press.
(7) Wang, Y.; Purrello, R.; Spiro, T. G. *J. Am. Chem. Soc.* **1989**, *111*, 8274–8276.

0002-7863/91/1513-6368$02.50/0

Another surprise is that the UVRR spectrum above 1200 cm^{-1} contains, in addition to the classical amide I, II, and III modes, extra bands at 1385 and 1495 cm^{-1}.[5-7] As discussed in the preceding paper,[8] the former band, labeled amide S, is due to a C–H bending mode, which gains its enhancement by vibrational mixing with the nearby amide III. The 1495-cm^{-1} band was attributed by Asher and Krimm and co-workers,[5] to the overtone of the amide V, N–H out-of-plane bending mode, whose fundamental was assigned at 748 cm^{-1} in the IR spectrum of aqueous NMA. Wang et al.,[7] however, have shown that this band is induced by the excitation laser. They assigned it instead to the amide II mode of the unstable cis isomer of NMA. In the present study, we confirm (as have Song et al.[6]) that the 1495-cm^{-1} band is laser-induced by showing that its intensity, relative to an internal standard, depends on the laser power. Its assignment to the cis isomer is established by comparison with the UVRR spectrum of the cyclic *cis*-amide caprolactam. The laser-induced effect is shown not to be a heating artifact by monitoring the temperature rise via the anti-Stokes intensity. Photoisomerization is weaker in acetonitrile than in water, and the extent of isomerization decreases in the order of NMA > *N*-ethylacetamide > glycylglycine; it is barely detectable for glycyllysine and alanylalanine. We have examined the NMA potential along the trans/cis twisting coordinate in the ground and first $\pi-\pi^*$ excited state with semiempirical MNDO/3 calculations. The calculated excited state has a minimum at an OCNH dihedral angle of 90°, suggesting a facile pathway for photoisomerization. The well depth is expected to increase for H-bonding solvents, accounting for the increased photoisomerization yield in water. The decreased isomerization for peptides is attributable to the steric clash of the C and N substituents when the C–N bond is twisted.

A search of the NMA UVRR spectrum under conditions in which photoisomerization is minimized failed to reveal significant enhancement of any band assignable to the amide V overtone, even directly on resonance with the amide $\pi-\pi^*$ transition, in contrast to the strong resonance enhancement of the twisting mode overtone in ethylene.[9] This difference in behavior can be related to differences in the nature of the excited states as well as in the nature of the normal modes.

Materials and Methods

The chemicals were purchased from Aldrich or Sigma (peptides) and used without purification. Most Raman samples were 5 mM in the molecule under study and contained 0.3 M Na_2SO_4 as an internal standard.

The UVRR spectrometer and H_2-Raman-shifted YAG laser source have been described elsewhere.[8,10] Excitation profiles were determined with samples in a sealed and stirred cuvette. The unsmoothed data were subjected to Lorentzian fitting of the RR bands for determination of band areas. No baseline correction was necessary. Interference from the 1640-cm^{-1} water band is serious only for the amide I band, and intensities were therefore determined for amide I′ in D_2O; the contribution of remnant H_2O in the D_2O samples was negligible. An unstirred cuvette was used for the laser-induced isomerization experiments, in which a steady state was established in 1–4 min, as judged from changes in the laser transmission. The isomerization induced in this way was reversible. There were no permanent changes in either the absorption or the UVRR spectra of samples after extended irradiation.

The MINDO/3 calculations were carried out with the MODPAC computational package (revision 2), running on a Micro-VAX 3400 computer.

Results and Discussion

A. H-Bonding Strongly Affects Amide Frequencies. As shown in Figure 1, the UVRR spectrum of NMA is markedly affected by the nature of the solvent. The highest frequency band is amide I, the mainly C–O stretching mode. Hudson and co-workers[2] noted that the amide I UVRR band, while strong in the gas phase or in acetonitrile, is barely detectable in water and suggested that it is strongly broadened by a distribution of H-bonded structures. The data of Figure 1, however, show a progressive downshift and weakening of amide I with increasing solvent polarity, from diethyl ether (spectrum c), to acetonitrile (spectrum b), to water (spectrum a), together with a simultaneous upshift and intensification of the next band, amide II. The near disappearance of amide I in water, underneath the nearby and much stronger amide II, is merely a continuation of this trend.

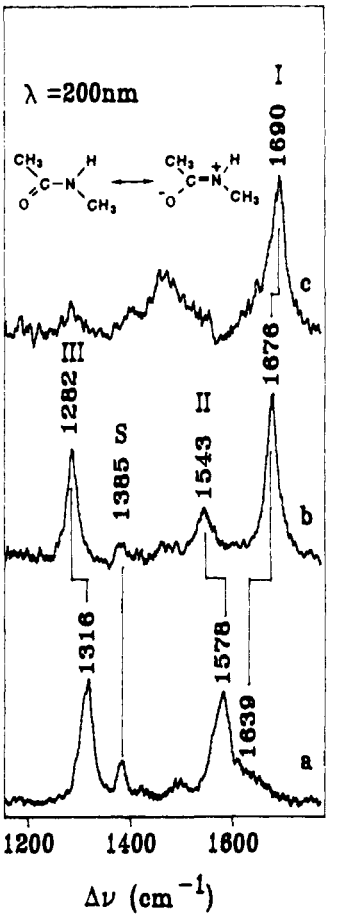

Figure 1. The 200-nm-excited UVRR spectra of NMA (5–10 mM) in (a) water, (b) acetonitrile-d_3, and (c) diethyl ether-d_{10}, illustrating the dramatic changes in the amide band frequencies and intensities with decreasing solvent acceptor number. Solvent bands have been subtracted out.

Between 1200 and 1400 cm^{-1} one finds the amide III and S bands. Amide II and III are coupled C–N stretching and N–H bending modes, while, as established in the preceding study,[8] amide S is a C_α–H bending mode which is in turn coupled with amide III. Amide III shifts to higher frequency between acetonitrile and water, by about the same amount as amide II, while the amide S frequency is nearly constant. Amide S gains intensity relative to amide III due to the stronger mixing when the two modes are closer in frequency. (In diethyl ether the amide II, III, and S intensities are sufficiently low, and the spectrum is sufficiently noisy, that assignments have not been made.) This behavior suggests that displacement along a single coordinate, presumably C–N stretching, is responsible for most of the resonance enhancement of all three modes. The resonance enhancement mechanism is discussed below, in connection with the excitation profiles.

The frequency trends can be understood in terms of the relative stabilities of the neutral and dipolar resonance forms of the amide bond, illustrated in Figure 1. Although the neutral form is the dominant one, the dipolar contribution is important, accounting for the planarity of the amide unit and the relatively high barrier to rotation about the C–N bond (see below). Polar solvents should increase the contribution of the dipolar resonance form, thereby

(8) Wang, Y.; Purrello, R.; Jordan, T.; Spiro, T. G. *J. Am. Chem. Soc.*, preceding paper in this issue.
(9) Sension, R.; Mayne, L.; Hudson, B. *J. Am. Chem. Soc.* **1987**, *109*, 5036–5038.
(10) Fodor, S. P. A.; Rava, R. P.; Copeland, R. A.; Spiro, T. G. *J. Raman Spectrosc.* **1986**, *17*, 471–475.

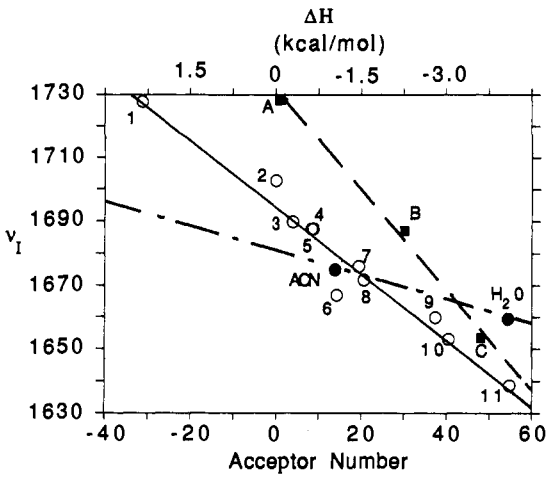

Figure 2. Correlation of the amide I frequency (cm^{-1}) with solvent acceptor number (circles) and interaction enthalpy (squares). The enthalpies are plotted for (A) NMA vapor ($\Delta H = 0$), (B) CCl_4, and (C) NMA dimer (with ν_1 for liquid NMA). The open circles are NMA frequencies in (1) vapor (this point is placed on the line in order to scale ΔH with acceptor number), (2) *n*-hexane, (3) di-*n*-butyl ether, (4) benzene, (5) CCl_4, (6) pyridine, (7) acetonitrile, (8) nitromethane, (9) ethanol, (10) liquid NMA, and (11) water. The NMA frequencies show *no* correlation with solvent donor number, as demonstrated in ref 11. The filled circles are frequencies for *N*-acetyltrialanine methyl ester in acetonitrile (ACN) and H_2O.

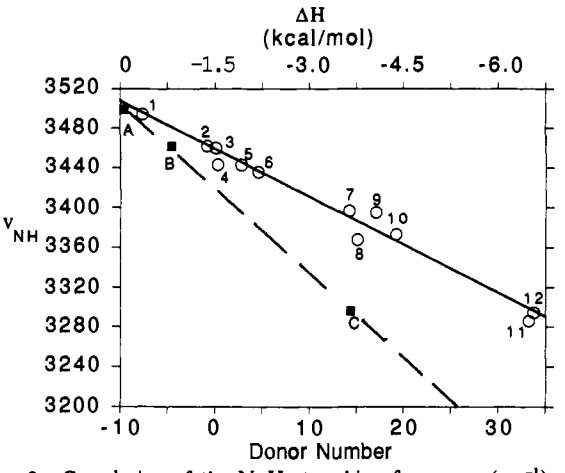

Figure 3. Correlation of the N–H stretching frequency (cm^{-1}) with solvent donor number (circles) and interaction enthalpy (squares). The enthalpies are plotted for (A) NMA vapor ($\Delta H = 0$), (B) $CHCl_3$, and (C) NMA dimer. The circles are NMA frequencies in (1) vapor (placed on the line to scale ΔH with donor number), (2) $CHCl_3$, (3) 1,2-dichloroethane, (4) benzene, (5) nitromethane, (6) nitrobenzene, (7) acetonitrile, (8) dioxane, (9) acetone, (10) diethyl ether, (11) pyridine, and (12) NMA liquid.

decreasing the C–O bond order and increasing the C–N bond order. This trend explains the concerted downshift in amide I and upshift in amide II and III, with increasing solvent polarity, as the C–O and C–N bonds are weakened and strengthened, respectively.

B. Carbonyl and N–H Interactions Are Independent. Surprisingly, however, the balance between the resonance structures is determined by interactions exclusively at the carbonyl group of NMA and not at the NH group. As shown in recent studies[11a,b] and illustrated in Figure 2, the NMA amide I frequency correlates linearly with the solvent acceptor number (AN), a measure of the tendency to accept electron pairs.[12] It does not correlate at all with the solvent donor number (DN),[11] a measure of the electron pair donating tendency,[12] as demonstrated in ref 11a. The correlation with AN is expressed by the equation

$$\nu_1\ (cm^{-1}) = a - b(AN) \qquad (1)$$

with $a = 1695.2$ and $b = 1.045$.

Donor solvents are expected, of course, to interact with the NH group, and Figure 3 shows that the frequency of the N–H stretching infrared band of NMA, obtained from the literature,[11c] correlates linearly with the solvent donor number, as expected. The equation is

$$\nu_{NH}\ (cm^{-1}) = c - d(DN) \qquad (2)$$

and $c = 3457.2$ and $d = 4.801$.

These data establish that interactions of the carbonyl and NH groups are uncorrelated and have no influence on one another. It might have been expected that the dipolar resonance form would be stabilized by NH as well as carbonyl H-bonding. The positive charge on the N atom is not as directly exposed to solvent as is the negative charge on the O atom, however. In addition, the H-bond from N–H affects the σ electron framework, to a first approximation, while H-bonds to the O atom can affect the π framework directly. These factors both reduce the sensitivity of the resonance structure to N–H interactions.

Because of this independence of carbonyl and N–H interactions, it is possible to gauge their strength directly from the vibrational data. To calibrate the vibrational frequency scales, we have used thermodynamic data on amides available from the literature. The enthalpy of interaction between dimethylformamide (DMF) and CCl_4 has been determined[12] to be −2.2 kcal/mol. DMF is an appropriate reference compound for NMA, since the slope of its amide I frequency correlation with solvent AN is the same as that for NMA.[11] Both molecules contain two methyl substituents, which apparently make the amide bond equally polarizable via interactions at the carbonyl group. DMF lacks an NH proton, however, so that the measured interaction enthalpy can be assumed to be exclusively determined by the carbonyl group and the acceptor properties of the solvent. In Figure 2, this enthalpy is plotted against the amide I frequency for NMA in CCl_4. Also included in the plot is the amide I frequency for gas-phase NMA,[2] for which the interaction enthalpy is zero, and of liquid NMA, against the NMA dimer interaction enthalpy, −3.5 kcal/mol.[13] These three points define a straight line

$$\nu_1\ (cm^{-1}) = e + f\Delta H\ (kcal/mol) \qquad (3)$$

with $e = 1729.5$ and $f = 20.6$. Equation 3 can be used to estimate the enthalpy for the NMA carbonyl H-bond in any medium from the amide I frequency.

In order to generalize this result to other amides, we need a connection between eqs 1 and 3, since enthalpy data are difficult to obtain, but the frequency dependence on AN can easily be determined. To do this we employ the gas-phase NMA amide I frequency to fix the AN scale in terms of enthalpy. As illustrated in Figure 2, AN = −31.4 for the gas phase, the negative value reflecting the fact that AN = 0 is defined by the acceptor properties of *n*-hexane. The intercept of eq 3 can then be written as $e = a - b(-31.4)$, while the slope is $f = br$, where r is the ratio of the two lines in Figure 2, $r = f/b = -19.7$. It is reasonable to expect that r and the gas phase AN are constant for all amides regardless of the nature of the substituent since these parameters merely adjust the ΔH and AN scales. On this assumption, ΔH can be estimated for any amide if the AN dependence of amide I has been determined. For example, Figure 2 also shows amide I frequencies for *N*-acetyltrialanine methyl ester in water and acetonitrile. These two points give $a = 1684.2$ and $b = -0.43$ in eq 1, and therefore $e = 1699.3$ and $f = -9.46$ in eq 3. Thus, the peptide carbonyl interaction enthalpy is estimated to be −4.3 and −2.6 kcal/mol in water and acetonitrile, respectively.

(11) (a) Grygon, C.; Spiro, T. G. *Biochemistry* **1989**, *28*, 4397. (b) Mohar, M. M.; Seehra, J. K.; Jagodzinski, P. *Spectrochim. Acta* **1989**, *44A*, 999. (c) Cutmore, E. A.; Hallam, M. E. *Spectrochim. Acta* **1969**, *25A*, 1767–1784.
(12) Gutman, V. *Coord. Chem. Rev.* **1976**, *18*, 225.
(13) Spencer, J. N.; Berger, S. K.; Powell, C. R.; Henning, B. D.; Furman, G. S.; Loffredo, W. M.; Rydberg, E. M.; Neubert, R. A.; Shoop, C. E.; Blauch, D. N. *J. Soln. Chem.* **1981**, *10*, 501.

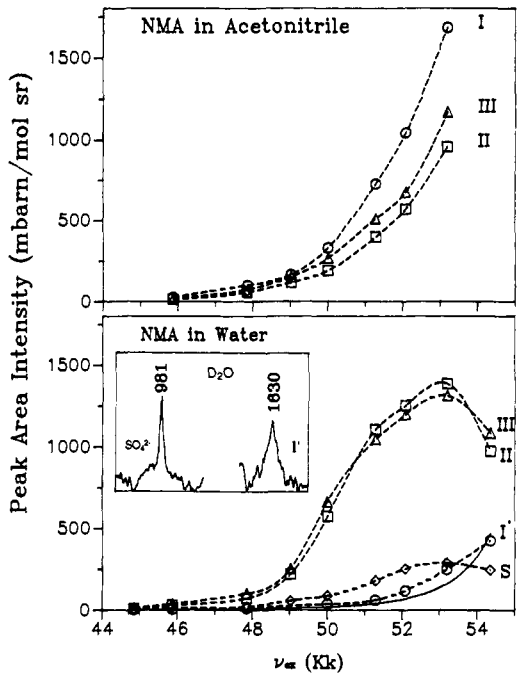

Figure 4. Excitation profiles (peak areas) for the amide I, II, III, and S bands of NMA in acetonitrile (top) and water (bottom). D_2O was used to determine the aqueous amide I′ profile and to eliminate interference from the 1640-cm^{-1} water band. The inset shows the amide I′ signal, relative to that of the sulfate internal standard (0.05 M NMA, 0.3 M SO_4^{2-}) with 200-nm excitation. The solid curve (bottom) is a fit of the amide I data to the A term expression for preresonance with a transition at 165 nm (see text).

A similar analysis of interaction enthalpies of the N–H H-bond can be carried out. In Figure 3, we plot N–H interaction enthalpies for NMA with $CHCl_3$, −0.8 kcal/mol,[13] and with itself (NMA dimer, −3.5 kcal/mol); the vapor phase serves as a third reference point ($\Delta H = 0$). For the NMA dimer interaction the C=O and N–H contributions are each equal to the total enthalpy, by definition. For NMA interacting with $CHCl_3$, the N–H contribution was obtained[13] by subtracting the C=O contribution, with DMF as a model compound. The three points define the line

$$\nu_1\ (\mathrm{cm}^{-1}) = g + h\Delta H\ (\mathrm{kcal/mol}) \qquad (4)$$

where $g = 3497.2$ and $h = 55.95$. Again, the DN scale can be converted to the enthalpy scale by noting that DN = −7.7 for the vapor phase (Figure 3); hence $g = c - d(-7.7)$, and $h = ds$ (where $s = h/d = -11.7$). The values of h and s should be properties of the group interacting with the N–H proton and can therefore be expected to apply to all amides.

C. Excitation Profiles Reveal Environmental Control of Excited States. Figure 4 shows excitation profiles (EPs) for the UVRR bands of NMA in water and in acetonitrile. (The dashed lines are drawn to connect the data smoothly, as a visual aid.) the intensities are plotted on an absolute scale, determined with reference to internal standard Raman bands of sulfate ion (981 cm^{-1}), present in the aqueous solution, or of acetonitrile (918 cm^{-1}). The acetonitrile intensities were scaled to those of sulfate,[14] with an aqueous solution containing 0.3 M Na_2SO_4 and 2 M acetonitrile; the resulting values were in good agreement with those of Dudik et al.[15] in the wavelength range, >220 nm, they reported. At the shortest wavelengths, 188 and 184 nm, the absolute intensity of sulfate has not been determined, and we used values predicted by the Albrecht A term fit to the data reported down to 192 nm.[14] The EPs are markedly solvent dependent. In water, the strongest band at all wavelengths is amide III, followed by amide II and amide S. All of them show EP maxima at 53.2 kK (188 nm), near coincidence with the NMA absorption band maximizing at 187 nm. The amide I band is weak, and its intensity was determined in D_2O, in order to shift the interfering amide II band out of the region; the signal quality of the amide I′ band is shown in the inset. It can be seen from Figure 4 that the amide I′ EP does not peak at 188 nm but continues to rise at the lowest available wavelength, 184 nm. The data can be fit (solid line) to the Albrecht preresonant A term dependence[17a]

$$\sigma_N = K(\nu_0 - \nu_N)^4 \left[\frac{\nu_e^2 + \nu_0^2}{(\nu_e^2 - \nu_0^2)^2}\right] \qquad (5)$$

with a resonant frequency, $\nu_e = 60.35$ kK ($\lambda_e = 165.7$ nm). This frequency is the same as that obtained earlier for the amide I band of polylysine.[17b]

In acetonitrile, however, the intensity order is reversed. At all wavelengths, amide I is the strongest band followed by amide III, amide II, and amide S. No peak is seen, the EPs showing a smooth rise to the shortest excitation wavelength, indicating a blue shift in the resonant electronic transition. The absorption maximum is also shifted to the blue in a less polar solvent.[16]

To understand these intensity effects, we examine the character of the resonant electronic transitions. The first two allowed transitions are expected to involve the amide π orbitals, of which there are three, constructed from the p_z orbitals (z is the direction perpendicular to the amide plane) on the N, C, and O atoms. These orbitals are illustrated in Figure 5, which is based on the orbital diagrams developed by Yan et al.[18] from extended Huckel (EHT) calculations. (The in-plane nonbonding orbital, centered on the O atom, has been omitted for clarity. This orbital is responsible for the very weak n–π^* transition at 210 nm, which does not contribute to the RR enhancement[3]). There are four π electrons, so the first two orbitals, π_1 and π_2, are filled, while the third, π_3, is empty; the two electronic transitions involve the orbital excitations $\pi_2 \rightarrow \pi_3$ and $\pi_1 \rightarrow \pi_3$. The first and third orbitals are primarily bonding and antibonding orbitals of the carbonyl group, while the middle orbital is primarily the N p_z orbital, with some contribution from the carbonyl orbitals. Consequently, the first allowed excited state, S_2 (S_1 is the n–π^* state, which lies lower), has charge transfer (N → O) character, while the second allowed state, S_3, can be described as a locally excited carbonyl state. Resonance with S_3 should therefore enhance the C–O stretching mode, amide I, primarily.

The enhancement pattern expected for resonance with S_2, however, depends on the π_2 orbital coefficients, which in turn depend on the energetics of the CO π and π^* orbitals with respect to the N p_z orbital. As noted by Yan et al.,[18] EHT calculations give a greater CO π^* contribution to the π_2 molecular orbital, while ab initio or CNDO/2 calculations give a greater CO π contribution. These alternative possibilities are diagrammed on the right and left side of Figure 5, respectively. When the CO π^* contribution is greater, the π_2 MO is antibonding with respect to the C–O bond but bonding with respect to the C–N bond. Therefore the π_2–π_3 orbital excitation should lengthen the C–N bond without a large affect on the C–O bond. Resonance enhancement would be expected for the amide II mode (and the coupled amide III and S modes), primarily. When the CO π contribution is greater, π_2 is bonding with respect to the C–O bond but antibonding with respect to the C–N bond. In that case, resonant enhancement of amide I should be greater than that of amide II, III, and S.

Both of these expectations are met experimentally, depending on the solvent. In water, amide II, III, and S, but *not* amide I, are enhanced in resonance with the first electronic transition, which has been assigned to the charge-transfer transition.[19] The amide

(14) Fodor, S. P. A.; Copeland, R. A.; Grygon, C. A.; Spiro, T. G. *J. Am. Chem. Soc.* **1989**, *111*, 5509.
(15) Dudik, J. M.; Johnson, C. R.; Asher, S. A. *J. Chem. Phys.* **1985**, *82*, 1732–1740.
(16) Nielson, E. B.; Schellman, J. A. *J. Phys. Chem.* **1967**, *71*, 2297.
(17) (a) Trulson, M. O.; Mathies, R. A. *J. Chem. Phys.* **1986**, *84*, 2068. (b) Copeland, R. A.; Spiro, T. G. *Biochemistry* **1987**, *26*, 2134.
(18) Yan, J. F.; Momany, F. A.; Hoffman, R.; Scheraga, H. A. *J. Phys. Chem.* **1970**, *74*, 420.

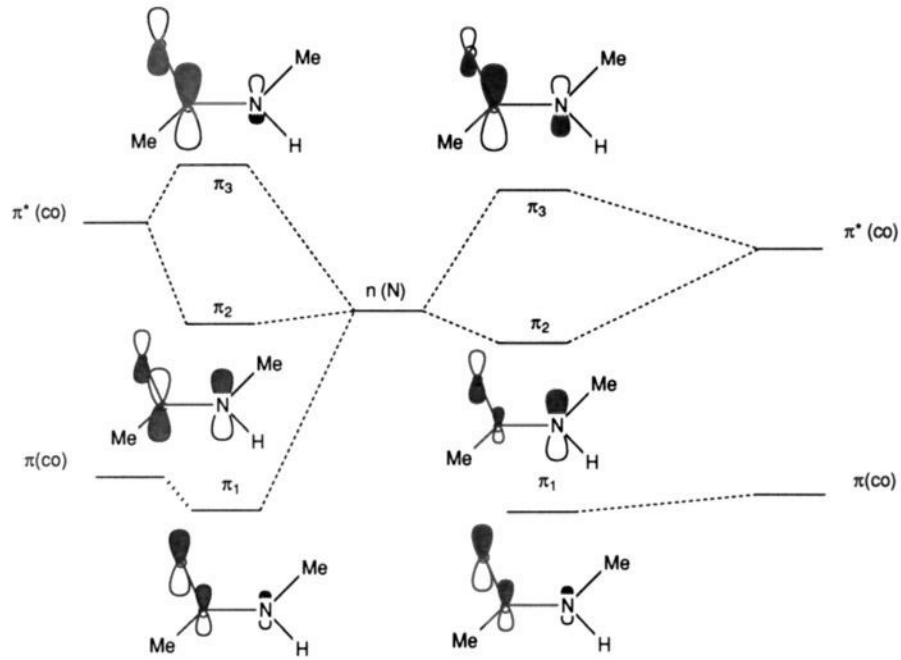

Figure 5. Orbital diagram for the two HOMOs of NMA, π_1 and π_2, and the first vacant π orbital π_3, illustrating the altered composition, especially of π_2, when the π^*(CO) fragment orbital is stabilized by H-bond donor interactions (right side).

I band is resonant with a higher lying transition, estimated from the A term plot to be at 165 nm. An absorption band near this wavelength has been assigned to the locally excited carbonyl transition.[17] Thus, the enhancement pattern in water is consistent with a dominant CO π^* contribution to the π_2 MO. In acetonitrile, however, the CO π contribution must be dominant, because the amide I band dominates the RR intensity, and is evidently resonant with the lowest allowed electronic transition, which, however lies at higher energy than in water. This upshift as well as the apparent reversal of the π_2 orbital composition makes good physical sense, because the CO π^* fragment orbital is expected to be lowered in energy, relative to the N p_z orbital, by H-bonding from water. The result should be a decrease in the π_2–π_3 energy gap (since π_3 is mainly CO π^* in character) as well as a dominant CO π^* (relative to CO π) contribution to π_2. This π^* dominance is an equivalent formulation of the dipolar resonance form dominance, which was invoked above to account for the amide vibrational frequency shifts in polar solvents. Thus, both the ground-state (frequencies) and excited-state (intensities) properties of the UVRR spectra can be explained qualitatively via stabilization of the CO π^* orbital by H-bond donors. It seems likely that the different results of ab initio vs EHT calculations with respect to the mixing coefficients of the CO π and π^* orbitals, reflect parameterization of the semiempirical EHT method on the basis of data from H-bonded crystals,[20a] so that the two sides of Figure 5 actually do represent H-bonding and apolar environments. This conjecture is strengthened by results which we obtained with EHT calculations in which the effect of solvents was modeled by systematically varying the input electronegativities of the O and N atoms. The orbital energies and coefficients changed in the manner shown in Figure 5.

We note that Nielson and Schellman[16] proposed that the absorption red-shift between cyclohexane and water is due to solvent interaction with the proton on the N atom, since the effect is greatest for primary amides, smaller for secondary amides, and is abolished for tertiary amides. They attributed the red-shift to stabilization of the charge-transfer excited state through N atom H-bonding. As demonstrated in the preceding section, however, solvent interaction with the N–H proton has essentially no effect on the amide electronic structure. The diminished cyclohexane–water red-shift on alkylation may alternatively be attributed to an increase in the p_z orbital energy due to alkylation of the N atom, which diminishes the HOMO–LUMO energy gap (Figure 5).

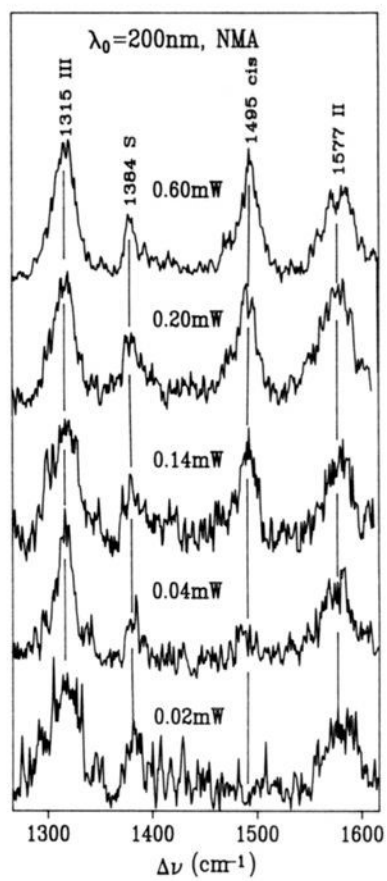

Figure 6. The 200-nm-excited UVRR spectra of aqueous NMA (5 mM) stationary sample in a quartz cuvette, with increasing average power (measured with a Scien Tech UV power meter) of the Raman laser. The spectra are scaled to roughly constant intensities of the amide III band.

(19) Kaya, K.; Nagakura, S. *Theor. Chim. Acta* **1967**, *7*, 117.
(20) (a) Momany, F. A.; McGuire, R. F.; Yan, J. F.; Scheraga, H. A. *J. Phys. Chem.* **1970**, *74*, 2424–2438. (b) Caprolatta, C.; Winkler, F. K.; Dunitz, J. D. *Acta Crystallogr.* **1975**, *B31*, 268.

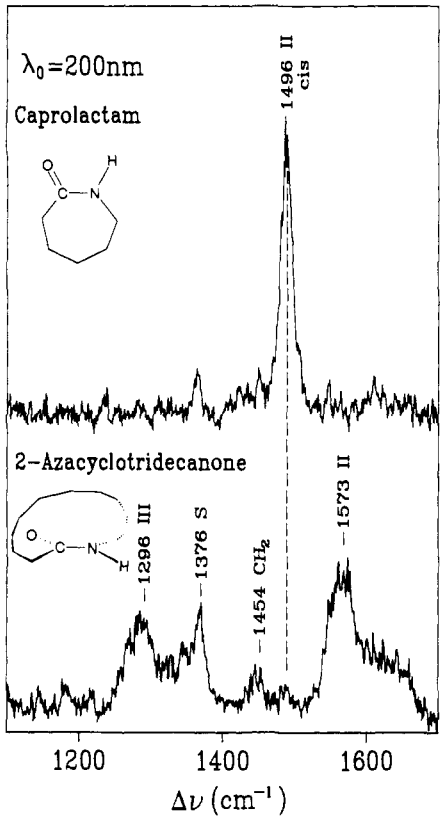

Figure 7. The 200-nm-excited UVRR spectra of the cyclic amides 2-azacyclotridecanone (13-membered ring) showing a typical *trans*-amide pattern and ε-caprolactam (7-membered ring) showing the collapse of most of the intensity into a single band, assigned to amide II of the cis isomer.

D. The 1495-cm^{-1} NMA UVRR Band Arises from Laser-Induced Cis Isomer. When the 200-nm-excited UVRR spectrum of aqueous NMA is obtained with a stationary sample, an additional band is observed at 1495 cm^{-1}, whose relative intensity is dependent on the laser power, as demonstrated in Figure 6. At the lowest average power, 0.02 mW, this band is barely detectable, but at 0.6 mW it is as strong as amide II and III. The effect is fully reversible, and the band disappears when the laser power is reduced again. It is barely detectable in a flowing sample (Figure 1), despite the high peak power of the laser pulses (~20 MW), so the quantum yield is low (Song et al.[6] estimate 0.09). At the same time the relaxation of the laser-induced species must be slow on the time scale of the interval between pulses, 0.1 s, in order to observe a buildup in the stationary samples. This buildup takes 1–4 min, as judged by changes in the transmission of the laser beam, after which a steady state is reached.

The 1495-cm^{-1} band is assigned to the cis isomer of NMA by comparing the UVRR spectra of caprolactam and 2-azacyclotridecanone (Figure 7). The latter is a 13-membered cyclic amide and shows a typical *trans*-amide pattern, with amide III, S, and II at 1296, 1376, and 1573 cm^{-1} (the weak 1454-cm^{-1} band is assigned to the CH_2 scissors mode of the 11 methylene groups, while the weaker 1496-cm^{-1} band indicates a small fraction of the cis isomer). In D_2O, these collapse to a single amide II′ band, at ~1500 cm^{-1} (not shown), as is also seen for NMA, due to the uncoupling of the C–N stretching and N–H bending coordinates. Caprolactam is a seven-membered cyclic amide; the smaller ring size enforces a cis conformation in solution (although a trans conformation is found in crystals[20b]). It shows a single strong UVRR band, at 1496 cm^{-1}, which undergoes only a 3-cm^{-1} downshift in D_2O. The near coincidence of the *cis*- and *trans*-amide II′ bands in D_2O with the cis band in H_2O, and the absence of cis bands attributable to amide III and S, implies unmixing of C–N stretching and N–H bending in the cis isomer, in contrast to the extensive mixing observed in the trans isomer. This unmixing is largely attributable to kinematic effects, as discussed in the preceding paper.[10] The coincidence of the caprolactam UVRR band with the laser-induced NMA band establishes that the latter arises from cis isomer; the band persists in D_2O solution,[7] as expected.

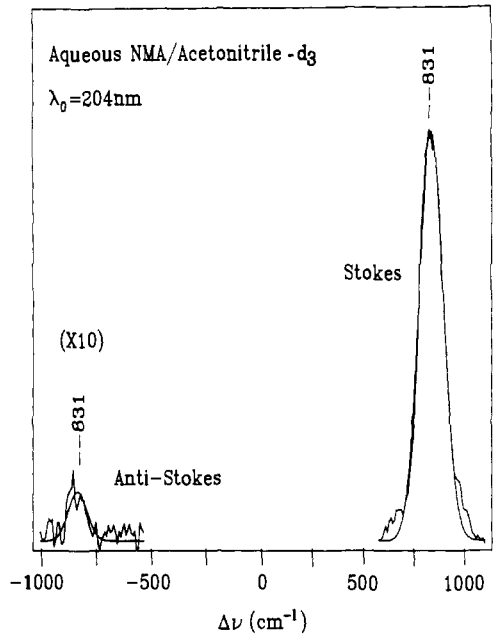

Figure 8. Stokes and anti-Stokes bands of the 831-cm^{-1} mode of deuterated acetonitrile (1.5 M) present as a probe molecule in an aqueous NMA (10 mM) stationary sample. The bands were fit to Lorentzian lines in order to compare their intensities (areas).

E. Isomerization Results from Photochemistry, Not Laser Heating. *cis*-NMA is only moderately unstable (2.5 kcal/mol[21,22]) with respect to the trans isomer. It is therefore conceivable that the laser-induced isomerization might result from a temperature rise upon irradiation of the UV-absorbing sample. To investigate this possibility, we measured the temperature with the Stokes/anti-Stokes intensity ratio of the 831-cm^{-1} Raman band of deuterated acetonitrile, added as a probe molecule to an aqueous NMA sample (Figure 8). A nonabsorbing probe molecule was employed rather than NMA itself, because the Stokes/anti-Stokes intensity ratio on resonance involves differing enhancement factors at the two scattering wavelengths and is therefore not straightforwardly related to the temperature.[23,24] For the probe molecule the temperature is given by the classical equation[25]

$$T = (h\nu/k)[\ln C(N_1/N_0) + 4 \ln (\nu_0 + \nu)/(\nu_0 - \nu)] \quad (6)$$

where ν_0 is the laser frequency, ν is the vibrational frequency, N_1/N_0 is the population ratio in the first excited and ground vibrational levels, given by the Stokes/anti-Stokes intensity ratio, and C is a self-absorption correction, which is given in ref 26 for the front sampling geometry of this experiment.

From the peak height ratio, 0.024, a temperature of 319 K is calculated, whereas the ambient temperature was 294 K. Thus, laser heating produced a 25 K temperature rise. This temperature rise results from the heat flow through the molecules in the scattering volume to the rest of the stationary sample over the time course of spectral acquisition (50 min) and may represent convective as well as diffusive dissipation between laser pulses. The temperature is expected to be the same for NMA as for the acetonitrile molecules, since vibrational relaxation of the photoexcited molecules is on the picosecond time scale while the laser pulses were 5 ns in duration.

(21) Jorgensen, W. L.; Gao, J. *J. Am. Chem. Soc.* **1988**, *110*, 4212.
(22) Stewart, W. E.; Siddal, T. H. *Chem. Rev.* **1970**, *70*, 517.
(23) Schomacker, K. T.; Champion, P. M. *J. Chem. Phys.* **1989**, *90*, 5982–5992.
(24) Alden, R. G.; Chavez, M. D.; Ondrias, M. R.; Courtney, S. H.; Friedman, J. M. *J. Am. Chem. Soc.* **1990**, *112*, 3241.

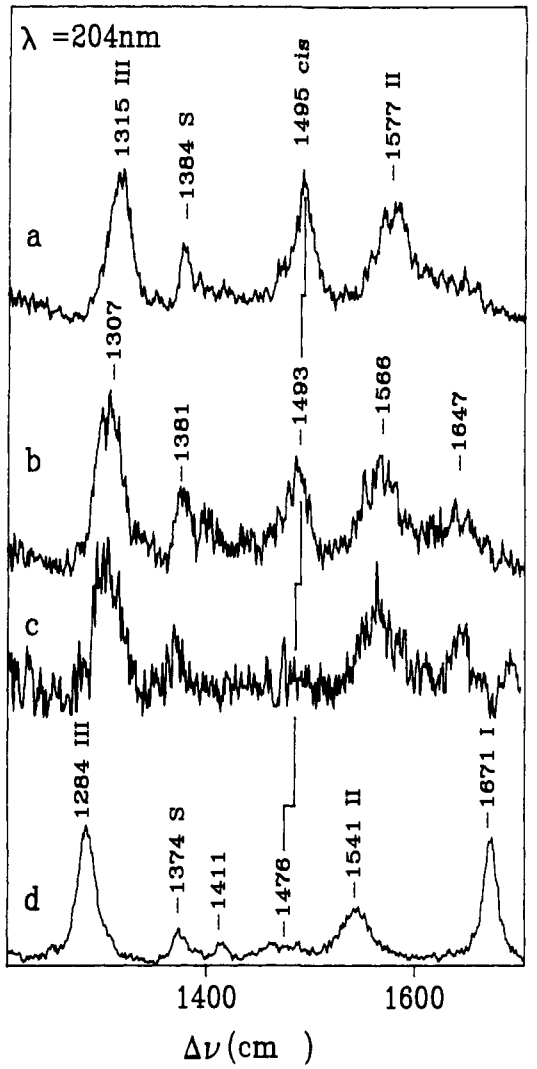

Figure 9. The 204-nm-excited UVRR spectra of stationary samples containing 5 mM NMA in (a) H_2O, (b) 50/50% volume mixture of H_2O/acetonitrile, (c) 20/80% mixture of H_2O/acetonitrile, and (d) pure acetonitrile, showing the decrease in photoinduced cis isomer with increasing acetonitrile content.

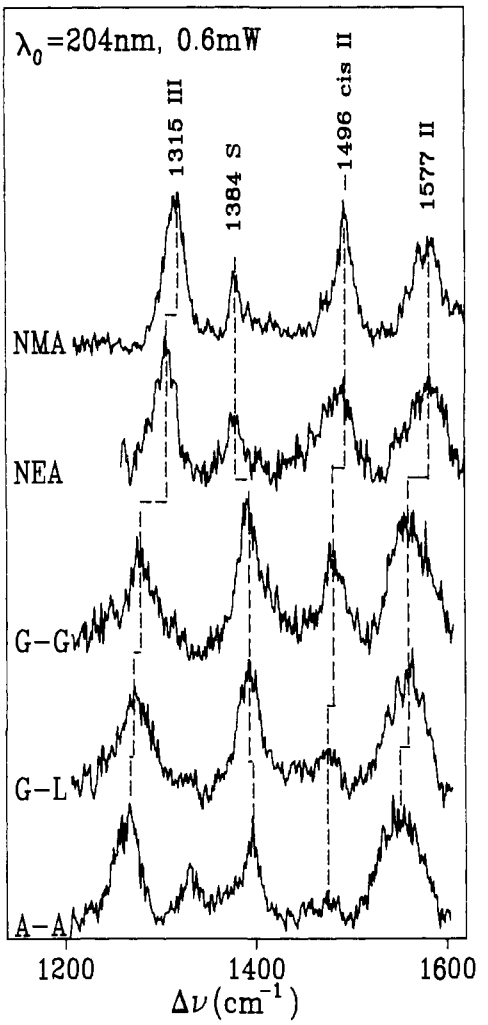

Figure 10. The 204-nm-excited UVRR spectra of stationary samples of aqueous NMA, *N*-ethylacetamide (NEA), glycyl-glycine (G-G), glycyl-lysine (G-L), and alanyl-alanine (A-A) (all 5 mM) taken at the same average power, 0.6 mW. Note the progressive elimination of the *cis*-amide II band.

NMR analysis indicates the equilibrium fraction of *cis*-NMA to be ~3% in aqueous solution at 298 K, giving a free energy difference of 2.5 kcal/mol.[21] The enthalpy difference should have about the same value since the entropy difference between the two isomers is expected to be small. The 25 K temperature rise should then produce an additional ~1% of cis isomer (consistent with experimental measurements of Song et al.[6]). The actual cis population was 20%, however, based on the 1495-1315-cm^{-1} peak height ratio of the NMA UVRR spectrum taken under identical conditions and assuming that the molar scattering factors of the two bands are the same as those in the spectrum of a 1/1 (mole ratio) mixture of caprolactam and NMA, obtained on a flowing sample. Thus, laser heating can only account for a small fraction of the observed isomerization, most of which is therefore attributable to photochemistry.

F. Polarity and Steric Influences on Photoisomerization. The photoisomerization yield is much higher for NMA in water than in acetonitrile, as seen in Figure 9, which compares UVRR spectra for stationary samples. The 1495-cm^{-1} *cis*-amide II band weakens, relative to the *trans*-amide II band, as the acetonitrile content of the sample increases and is barely detectable in pure acetonitrile. (Both bands shift down in frequency in the less polar solvent, as expected.) Part of the intensity loss might be due to the blue-shift of the electronic absorption band in acetonitrile (see previous section), resulting in a lower fraction of photoexcited molecules. The absorptivity at the excitation wavelength, 204 nm, is only ~2-fold lower in acetonitrile than in water, however. Moreover, we were unable to increase the *cis*-amide II intensity in acetonitrile by increasing the laser power, so that the vanishingly low yield of the cis isomer cannot be explained by the absence of photoexcitation.

Large changes in the photoisomerization yield are also seen when the substituents on the C and/or N atoms of the amide bond are altered. Figure 10 compares UVRR spectra for stationary aqueous samples of NMA, NEA (*N*-ethylacetamide), and three dipeptides, all with the same incident laser power, 0.6 mW. The dipeptides show the same amide II, S, and III band pattern as NMA and NEA, although the frequencies are somewhat shifted. The 1496-cm^{-1} cis band, however, has significant intensity for glycylglycine only and can barely be seen for glycyllysine and alanylalanine. The relative intensity of the 1495-cm^{-1} band is lower for glycylglycine than for NEA, which is in turn lower than for NMA. Thus, the photoisomerization yield is related to the size of the substituents on the C and N atoms of the amide bond. Figure 11 shows similar reductions in the cis photoisomerization yield when the H atoms of the carbonyl methyl group of NMA are successively replaced by methyl groups. The first replacement (*N*-methylpropionamide) lowers the cis band intensity slightly, while the second replacement (*N*-methylisobutyramide) has a larger effect. Photoisomerization is undetectable when all three H atoms are replaced (*N*-methylpivaloylamide).

In Figure 12, the intensity of the 1495-cm^{-1} band, relative to that of the *trans*-amide II band, is plotted against the average laser power at 204 nm. The cis/trans population ratio rises at

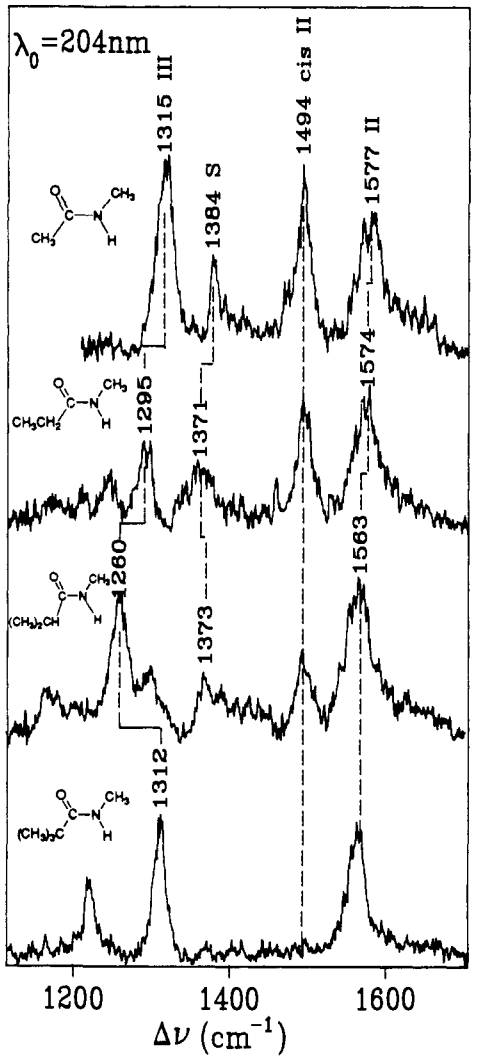

Figure 11. The 204-nm-excited UVRR spectra of stationary samples of aqueous NMA, *N*-methylpropionamide, *N*-methylisobutyramide, and *N*-methylpivalamide (5 mM) at the same average power, 0.5 mW. The *cis*-amide II band diminishes with increasing steric bulk of the amide substituent and disappears for *N*-methylpivalamide.

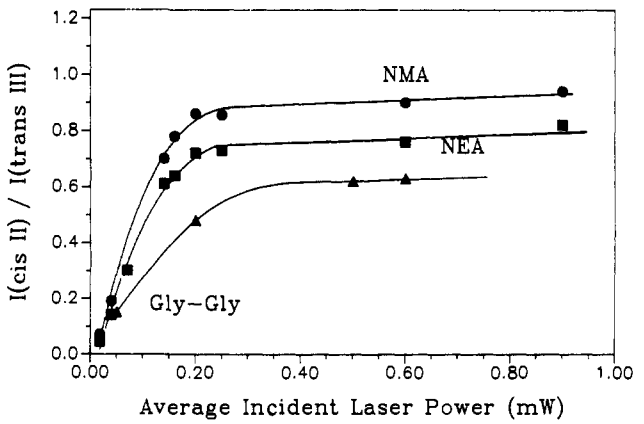

Figure 12. Intensity ratio of the *cis*-amide II and *trans*-amide III bands for stationary samples of NMA, NEA, and glycyl-glycine, as a function of increasing laser power at 204 nm.

low power and then levels off, showing saturation behavior. At this point, the trans → cis isomerization rate is balanced by the cis → trans rate.

G. Twisting Potential in the Ground and Excited States. To explore the amide photoisomerization process further, we have calculated the NMA potential as a function of twisting about the C–N bond in the ground and first singlet $\pi-\pi^*$ (S_2) excited states,

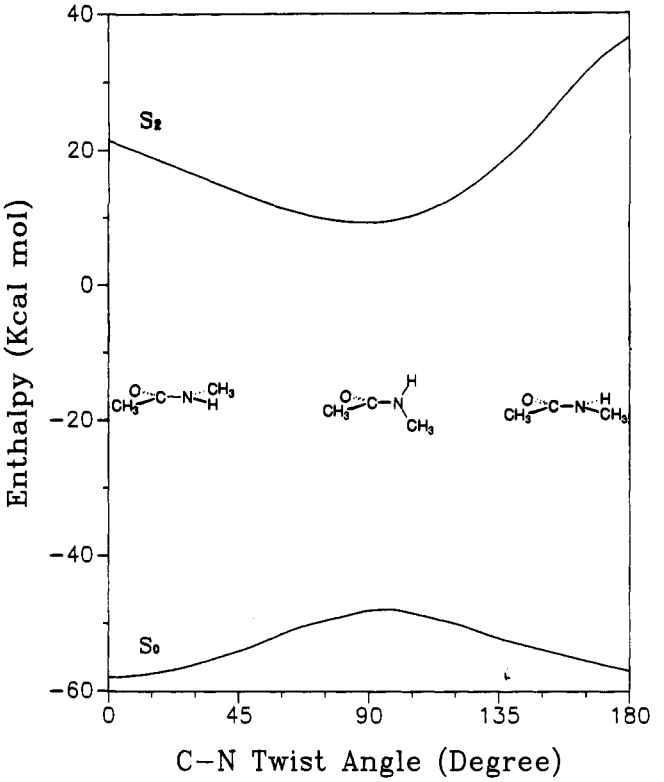

Figure 13. MINDO/3-calculated twisting potentials for the ground and first $\pi-\pi^*$ excited state of NMA. The trans (0°), cis (180°), and 90° geometries are shown.

with the MNDO/3 semiempirical method.[27] The results are shown in Figure 13. Hoesterey et al.[28] have previously reported the NMA ground-state twisting potential calculated with MINDO/3, and our results are in agreement with theirs. The cis–trans enthalpy difference is 1.4 kcal/mol, in reasonable agreement with the 2.5-kcal/mol estimate of the free energy difference from NMR data[22] and ab initio calculations.[21] A 12-kcal/mol barrier is calculated at a twist angle of 90°, somewhat lower than the 20-kcal barrier determined via NMR for NMA in D_2O.[22] However, the barrier is likely to be very sensitive to the polarity of the medium, as discussed below. Even the planar NMA structure is sensitive to the environment (see Discussion in the preceding article), as is readily seen in the experimentally determined C–N bond length, which is 1.40 Å in the gas phase,[29a] but only 1.25 Å in the crystal phase,[29b] in which there are intermolecular H bonds. The MINDO/3 calculation gives an intermediate value, 1.36 Å. Although the calculation is carried out on an isolated NMA molecule, it is likely that the parameters in the program, obtained from experimental data on a variety of molecules,[27] produce an effective polarity that is greater than that of the vacuum.

The calculated excited-state potential shows a minimum at 90°. There are several things wrong with this potential, however. The large calculated cis–trans energy difference is implausible, since the C–N bond is lengthened in the excited state, and steric factors should be attenuated. Indeed, the absorption spectrum of caprolactam is red-shifted (5 nm) relative to NMA, suggesting that the cis structure is stabilized relative to the trans structure in the excited relative to the ground state. The calculated S_0–S_2 energy difference for *trans*-NMA, ~80 kcal/mol, is also much less than expected from the vertical excitation energy (188 nm, 148 kcal/mol). Finally, the finite slope at zero twist angle is incorrect,

(25) Long, D. A. *Raman Spectroscopy*; McGraw-Hill: New York, NY, 1977; p 77.
(26) Fodor, S. P. A.; Rava, R. P.; Hays, T. R.; Spiro, T. G. *J. Am. Chem. Soc.* **1985**, *107*, 1520.
(27) Bingham, R. C.; Dewar, M. J. S.; Lo, D. H. *J. Am. Chem. Soc.* **1975**, *97*, 1285.
(28) Hoesterey, B.; Neely, W. C.; Worley, S. D. *Chem. Phys. Lett.* **1983**, *94*, 311.

since the potential must be symmetric about the planar geometry. It is possible, that the upper state actually has a local minimum at the planar geometry, as has indeed been established for the photoexcited state of stilbene.[30a,b] The semiempirical potential is offered only to illustrate the plausibility of photoisomerization via a twisted excited state. A very recent ab initio calculation confirms that the S_2 state is twisted.[31]

Polarity effects on the C–N bond twisting potential can be understood qualitatively in terms of the same orbital mixing arguments given above to explain the RR frequencies and intensities. By stabilizing the CO π^* orbital, H-bonding solvents increase the C–N bonding character of the HOMO and also the C–N antibonding character of the LUMO (Figure 5). (Equivalently, the dipolar resonance form is enhanced in the ground state but suppressed in the excited state.) Consequently, the well depth of the S_1 twisting potential should deepen. This can account for the greater photoisomerization yield in water than in acetonitrile.

Steric effects can be understood on the basis of the clash between C and N substituents when the C–N bond is twisted by 90°. This clash is expected to add an angle-dependent term to the twisting potential, which should rise the energy at 90° for both the ground and excited states. The effect would be to displace the excited-state minima from 90°, thereby reducing the photoisomerization probability. The steric suppression of photoisomerization is detectable for NEA, relative to NMA, and is more pronounced for glycylglycine. In this simplest dipeptide the N substituent is the acetate group, with a size similar to the ethyl group of NEA, while the C substituent is the aminomethylene group, which is larger than the methyl group of NEA. Amino acids other than glycine have bulky substituents, R, on the C_α atom next to the C atom. It is therefore not surprising that even for alanylalanine (R = methyl) photoisomerization is undetectable.

Apparently only glycine is a candidate for photoisomerization in polypeptides. Moreover, it is reasonable to expect that glycine residues would have sufficient mobility to photoisomerize only when they are at the termini of a polypeptide chain. To investigate this question, we examined the UVRR spectrum of a stationary sample of hexaglycine (not shown) and found that the photoinduced *cis*-amide band had only about 40% of the intensity, relative to the unisomerized *trans*-amide II band, of the diglycine sample, consistent with only the outer two of the five peptide bonds in hexaglycine being subject to photoisomerization. Thus, photoisomerization is unlikely to be a significant problem in the UVRR spectroscopy of polypeptides and proteins.

H. Absence of Amide V Overtone Enhancement. Since the S_1 state is stabilized by twisting about the amide C–N bond, the normal modes with large contributions from the C–N twisting coordinate should be active in the UVRR spectrum. These modes destroy the symmetry plane of the amide chromophore, so their fundamentals are Raman-forbidden, but the overtones and other even-quantum harmonics are Raman-allowed and should be enhanced via resonance with the S_1 transition. In ethylene, the first twisting mode overtone, at $\sim$2080 cm^{-1}, is strongly enhanced with excitation at 175 nm in resonance with its first allowed transition, and several even harmonics are also seen.[8] It was this analogy that led Song et al.[5] to propose an amide V overtone assignment to the 1495-cm^{-1} band which they observed in the 220-nm-excited RR spectrum of NMA, since the fundamental has been assigned from IR spectra at 725 cm^{-1} in liquid NMA[32] and at 748 cm^{-1} in aqueous solution. Amide V is mainly N–H out-of-plane bending in character[32] and should promote twisting about the C–N bond. The 1495-cm^{-1} band is now reassigned to amide II of the photoinduced cis isomer, and the other conceivable candidate band,[7] at 1395 cm^{-1}, is now assigned to amide S.[8] Thus, the UVRR spectrum lacks any prominent band assignable to the amide V overtone.

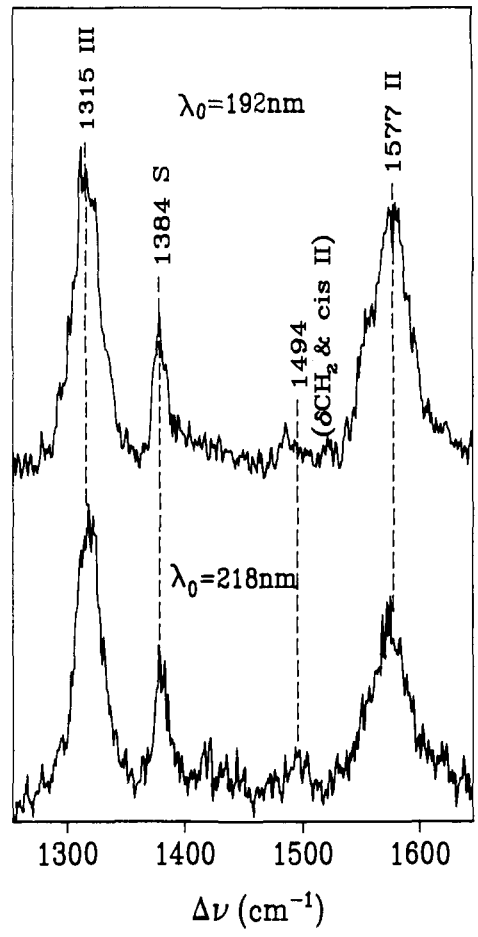

Figure 14. Comparison of aqueous NMA UVRR spectra with 192- and 218-nm excitation.

Since the excitation profiles of overtones are more sharply peaked at resonance than those of fundamentals,[33] we searched for additional candidates with 192-nm excitation, close to resonance with the first absorption maximum of aqueous NMA. The spectrum at this wavelength, although stronger overall, shows no new features (Figure 14). A weak band is seen at 1495 cm^{-1} which is attributable to equilibrium cis isomer.[6] It shows no relative intensity gain at 192 nm with respect to 218 nm, so any contribution of the amide V overtone must be very small.

We therefore conclude that the amide V overtone is not significantly enhanced. The likeliest explanation is that the excited-state potential has a local minimum at the planar geometry and that there is a barrier to twisting. In that case, enhancement would be weak[34] since the change in the C–N torsional force constant upon vertical excitation would be small. The ab initio calculation of Li et al.[31] does indicate a barrier in the S_2 state. Alternatively, there may be dynamical processes that suppress the intensity, e.g., rapid relaxation of the torsional levels in the excited state.

An additional consideration is that amide V is not a purely C–N twisting mode.[32] Displacement of the N–H bond out of the plane leads to pyramidalization of N as well as C–N twisting. Also, the presence of heavy atom substituents (the carbonyl O and the two methyl groups) changes the twisting dynamics materially. For ethylene, with exclusively H atom substituents, the relatively high-frequency hydrogenic mode at 1044 cm^{-1} is the *only* normal coordinate for C–C twisting.[8] In NMA, however, the out-of-plane displacement of the O and C substituent atoms are expected to contribute more to C–N twisting than the H-atom displacement.

(29) (a) Costain, C. C.; Dowling, J. M. *J. Chem. Phys.* **1960**, *32*, 158. (b) Kimura, M.; Aoki, M. *Bull. Chem. Soc. Jpn.* **1953**, *26*, 429.
(30) (a) Felker, P. M.; Zewail, A. H. *J. Phys. Chem.* **1985**, *89*, 542. (b) Amirav, A.; Sonnenschein, M.; Jortner, J. *J. Chem. Phys.* **1984**, *88*, 199.
(31) Li, Y.; Garrel, R. L.; Houk, K. N. Submitted for publication.
(32) Krimm, S.; Bandekar, J. *Adv. Prot. Chem.* **1986**, *38*, 181–364.
(33) Sension, J.; Hudson, B. *J. Chem. Phys.* **1989**, *90*, 1377–1389.
(34) Myers, A. B.; Mathies, R. A. *Biological Applications in Raman Spectroscopy*; Spiro, T. G., Ed.; John Wiley & Sons, New York, 1987; pp 1–58.

This consideration suggests that a search of the low-frequency UVRR spectrum might yield evidence for C-N twisting overtone enhancement.

Conclusions

UVRR spectroscopy of NMA shows the amide bond to be strongly affected by the electron-acceptor (or H-bond donor) properties of its environment, in both the ground and first $\pi-\pi^*$ excited states. The observed affects can be understood as resulting from stabilization of the C=O π^* fragment orbital by electron-acceptor interactions, and the consequent introduction of C-O antibonding and C-N bonding π character into the HOMO. The result is a frequency decrease for the amide I C-O stretching mode which is linearly dependent on the solvent acceptor number, and a frequency increase in the amide II and III modes which share the C-N stretching coordinate. H-bond acceptor interactions at the N-H bond have no affect on the amide frequencies but decrease the N-H stretching frequency in proportion to the solvent donor number. Apparently, the N-H and C=O H-bond interactions are effectively insulated from one another by the $\pi-\sigma$ separation. This insulation makes it possible to evaluate the energetics of C=O and N-H H-bonds independently from spectroscopic data.

The C=O π^* stabilization by electron-acceptor interactions also introduces C-N antibonding character into the first vacant π^* molecular orbital, while retaining C-O antibonding character. Consequently, the excited-state potential is displaced more along the C-N stretching coordinate and less along the C-O stretching coordinate, with the result that amide II and III are intensified, as is amide S via its coupling to amide III, while amide I is weakened. Indeed, in water, amide I shows no resonance enhancement from the first π^* excited state but only from the second, which is mainly a C-O localized state.

The first π^* excited state is also expected to distort by twisting about the C-N bond and to have a minimum energy at a 90° twist angle, thereby providing a pathway for the photoisomerization which is readily observed for NMA via UVRR spectroscopy. This effect should be accentuated by H-bond donor interactions, due to the same orbital composition changes, as is evident from the increasing photoisomerization yield with increasing water content of water/acetonitrile mixtures. The photoisomerization yield decreases with increasing steric bulk of the C and N substituents and is expected to be negligible for polypeptides, except for terminal glycine residues.

While the twisting distortion in the excited state should enhance even quantum transitions of twisting modes in the UVRR spectra, the amide V N-H out-of-plane overtone is undetectable even directly on resonance with the first π^* transition. The likelist explanation is that the change in the C-N torsional force constant is minimized by a barrier to twisting in the excited state and also that the extent of C-N twisting in this mode is relatively small. Low-frequency modes involving out-of-plane displacements of the carbon substituents may be better candidates for overtone enhancement.

Acknowledgment. We thank Professors Krimm and Asher and Professors Garrel and Houk for communicating results of their work prior to publication. This work was supported by NIH Grant GM 25158.

Registry No. NMA, 79-16-3; NEA, 625-50-3; G-G, 556-50-3; G-L, 997-62-6; A-A, 1948-31-8; H_3CCN, 75-05-8; EtOEt, 60-29-7; $H_3C(CH_2)_4CH_3$, 110-54-3; BuOBu, 142-96-1; PhH, 71-43-2; CCl_4, 56-23-5; H_3CNO_2, 75-52-5; EtOH, 64-17-5; $CHCl_3$, 67-66-3; $ClCH_2CH_2Cl$, 107-06-2; $PhNO_2$, 98-95-3; H_3CCOCH_3, 67-64-1; *N*-methylpropionamide, 1187-58-2; *N*-methylisobutyramide, 2675-88-9; *N*-methylpivalamide, 6830-83-7; hexaglycine, 3887-13-6; pyridine, 110-86-1; dioxane, 123-91-1; 2-azacyclotridecanone, 947-04-6; ε-caprolactam, 105-60-2.

Temperature Coefficients of the Rates of Cl Atom Reactions with C_2H_6, C_2H_5, and C_2H_4. The Rates of Disproportionation and Recombination of Ethyl Radicals

Otto Dobis† and Sidney W. Benson*

Contribution from Loker Hydrocarbon Research Institute, University of Southern California, University Park, Los Angeles, California 90089-1661. *Received November 5, 1990*

Abstract: Using the very low pressure reactor (VLPR) with recent improvements, we have been able to measure the following rate constants over the range 203-343 K: $Cl + C_2H_6 \xrightarrow{1} HCl + C_2H_5$, $k_1 = (8.20 \pm 0.12) \times 10^{-11} \exp[(-170 \pm 20)/RT]$; $Cl + C_2H_5 \xrightarrow{2} HCl + C_2H_4$, $k_2 = (1.20 \pm 0.08) \times 10^{-11}$; $2C_2H_5 \xrightarrow{3} C_2H_4 + C_2H_6$, $k_3 = (2.00 \pm 0.06) \times 10^{-12}$; $Cl + C_2H_4 \xrightarrow{4} HCl + C_2H_3$, $k_4 = (1.15 \pm 0.13) \times 10^{-10} \exp[-3200 \pm 140)/RT]$. All rate constants are in units of cm^3/molecule·s and energies are in cal/mol. Reactions 2 and 3 have no observable temperature dependence over the range measured. Combining k_3 with the experimentally measured value of the ratio of recombination to disproportionation of 0.14 ± 0.01, also independent of temperature, yields for the rate of recombination of ethyl radicals: $k_r = (1.42 \pm 0.11) \times 10^{-11}$. Combining the values of k_4 with the previously measured values of the equilibrium constant K_4 and third law corrected values of ΔS_4 gives for the back reaction: $k_{-4} = (8.7 \pm 0.3) \times 10^{-13} \exp[(-200 \pm 200)/RT]$ and $\Delta H°_{298}(C_2H_3\text{-}H) = 106.0 \pm 0.3$ kcal/mol. The absence of any measurable butane shows that the recombination rate is at least a factor of 400 below its high-pressure value at 3 mTorr. Mass spectral sensitivity data for ethyl radical between 29 and 25 amu is also reported for 20 and 40 eV.

Introduction

Recent improvements[1,2] in the very low pressure reactor (VLPR) have made it possible to study very fast atom-molecule reactions over an extended temperature range, -80 to 200 °C. The reaction of $Cl + C_2H_6$ at room temperature has recently been explored[2] and shown to consist of a number of consecutive and concurrent radical-radical as well as radical-molecule reactions. The entire reaction scheme together with measured rate constants at 298 °K is shown in Scheme I.

† Present address: Technical University, H-1521 Budapest, Hungary.

(1) Dobis, O.; Benson, S. W. *Int. J. Chem. Kinet.* **1987**, *19*, 691.
(2) Dobis, O.; Benson, S. W. *J. Am. Chem. Soc.* **1990**, *112*, 1023.

0002-7863/91/1513-6377$02.50/0